PNAS RESEARCH ARTICLE | PLANT BIOLOGY OPEN ACCESS

# *GRASSY TILLERS1* (*GT1*) and *SIX-ROWED SPIKE1* (*VRS1*) homologs share conserved roles in growth repression

Joseph P. Gallagher[a,b,1], Jarrett Man[a], Adriana Chiaramida[a], Isabella K. Rozza[a], Erin L. Patterson[a], Morgan M. Powell[a], Amanda Schrager-Lavelle[a], Dilbag S. Multani[c,d], Robert B. Meeley[c], and Madelaine E. Bartlett[a,1]

Edited by James Birchler, University of Missouri, Columbia, MO; received July 21, 2023; accepted October 31, 2023

**Crop engineering and de novo domestication using gene editing are new frontiers in agriculture. However, outside of well-studied crops and model systems, prioritizing engineering targets remains challenging. Evolution can guide us, revealing genes with deeply conserved roles that have repeatedly been selected in the evolution of plant form. Homologs of the transcription factor genes *GRASSY TILLERS1* (*GT1*) and *SIX-ROWED SPIKE1* (*VRS1*) have repeatedly been targets of selection in domestication and evolution, where they repress growth in many developmental contexts. This suggests a conserved role for these genes in regulating growth repression. To test this, we determined the roles of *GT1* and *VRS1* homologs in maize (*Zea mays*) and the distantly related grass brachypodium (*Brachypodium distachyon*) using gene editing and mutant analysis. In maize, *gt1; vrs1-like1* (*vrl1*) mutants have derepressed growth of floral organs. In addition, *gt1; vrl1* mutants bore more ears and more branches, indicating broad roles in growth repression. In brachypodium, *Bdgt1; Bdvrl1* mutants have more branches, spikelets, and flowers than wild-type plants, indicating conserved roles for *GT1* and *VRS1* homologs in growth suppression over *ca.* 59 My of grass evolution. Importantly, many of these traits influence crop productivity. Notably, maize *GT1* can suppress growth in arabidopsis (*Arabidopsis thaliana*) floral organs, despite *ca.* 160 My of evolution separating the grasses and arabidopsis. Thus, *GT1* and *VRS1* maintain their potency as growth regulators across vast timescales and in distinct developmental contexts. This work highlights the power of evolution to inform gene editing in crop improvement.**

sex determination | evo-devo | HD-ZIP transcription factors | tillering | inflorescence development

## Significance

During plant evolution and domestication, some genes are repeatedly targeted by selection to sculpt development and influence crop productivity. For example, in maize, barley, and many other grass crops, grain production is affected by growth suppression in floral organs. This growth suppression is controlled by class I HD-ZIP transcription factors, which have been repeatedly selected to suppress growth, suggesting deep conservation of function. We found that HD-ZIP transcription factors GT1 and VRL1 regulate growth suppression in branching and flowering structures in maize and brachypodium. Our findings confirm that these two gene lineages share a conserved role in growth suppression and demonstrate how evolution and domestication can be used to predict strong gene editing targets for crop improvement.

Gene editing is a powerful tool for improvement of major crops and de novo domestication of weakly domesticated crops and wild crop relatives (1–9). Virtually all crops stand to benefit from this targeted approach to crop development and improvement. However, selecting the best targets for editing can be challenging outside of model systems and well-studied crops and plant families. Luckily, evolution has already selected many strong targets for modifying crop traits.

Conservation of function and regulatory patterns can guide the selection of gene editing targets. Some gene families regulate similar functions in plant development across species and have been repeatedly selected to modify similar processes under domestication (10, 11). Importantly, conserved gene function means that insights regarding these genes might be translated from model systems to other species with greater confidence. For example, gene editing of the conserved *CLAVATA* (*CLV*)–*WUSCHEL* (*WUS*) meristem homeostasis pathway and the flowering time-regulating *FLOWERING LOCUS T* (*FT*)/*TERMINAL FLOWER1* (*TFL1*) family genes has improved yield traits in maize and tomato and accelerated domestication of wild relatives and weak domesticates (1, 3, 5, 12–16). Regulatory patterns may also be a useful metric for choosing targets for gene editing. For example, targeting negative regulators may be more effective than targeting positive regulators. Reduced function mutants are easier to generate than gain of function mutants via gene editing (17). Thus, targeting negative regulators will likely enhance the function that is normally suppressed. Gene-edited alleles of genes encoding negative regulators, such as *CLV1* and *CLV3* homologs (12, 14), *FT*/*TFL1* homologs (3, 18, 19), and the rice grain size gene *GS3* (2, 4), have all led to improvement of important agronomic traits. Genes that encode negative regulators, in addition to having conserved function across deep time, could be particularly effective targets in gene editing for crop improvement and de novo domestication.

The class I homeodomain-leucine zipper (HD-ZIP) transcription factors meet these criteria. One class I HD-ZIP gene is the barley (*Hordeum vulgare*) domestication gene *SIX-ROWED SPIKE1* (*VRS1*). Grass flowers are held in specialized branching structures called spikelets. Modifying spikelet development was key in barley domestication (20). Barley spikelets occur in sets of three, one central spikelet and two lateral spikelets, on each node of the inflorescence main axis, the rachis. Each spikelet contains a single flower

This manuscript was submitted to preprint server biorxiv under the CC-BY-NC-ND 4.0 International license. The DOI is https://doi.org/10.1101/2023.03.15.532786.

Author contributions: J.P.G., J.M., and M.E.B. designed research; J.P.G., J.M., A.C., I.K.R., E.L.P., M.M.P., and A.S.-L. performed research; J.P.G., D.S.M., and R.B.M. contributed new reagents/analytic tools; J.P.G. analyzed data; and J.P.G. and M.E.B. wrote the paper.

The authors declare no competing interest.

This article is a PNAS Direct Submission.



[1]To whom correspondence may be addressed. Email: joseph.gallagher@usda.gov or mbartlett@umass.edu.

This article contains supporting information online at https://www.pnas.org/lookup/suppl/doi:10.1073/pnas.2311961120/-/DCSupplemental.

Published December 14, 2023.

that develops a pistil, the ovule-bearing structure, and stamens, the pollen-bearing structures. However, the two lateral spikelet flowers are normally sterile, lacking pistils due to growth suppression, while the central spikelet maintains its fertility (21). In the barley mutant *vrs1*, the lateral spikelet pistils are derepressed and develop into fertile pistils that can form grains (20). Interestingly, an alternate allele of *VRS1* increases repression of pistil development in lateral spikelets and produces a larger mature grain in the central spikelet than wild type, demonstrating that growth repression is a core function of this gene (22). Mutants of the *VRS1* homologs in other species also display reduced growth repression. Variants in *GRAIN NUMBER INCREASE1 (GNI1)* increased yield in durum wheat (*Triticum turgidum*) and bread wheat (*T. aestivum*) through an increase in the number of fertile flowers per spikelet (23). Similarly, mutant alleles of the co-orthologs of *VRS1* increase kernel row number in maize, albeit through an unknown developmental mechanism (24). Barley *vrs1* mutants also develop larger leaves, though fewer tillers, suggesting that this gene can affect more than reproductive structures (25, 26). Thus, *VRS1* and its homologs regulate plant growth suppression in various contexts in several grass species.

Many class I HD-ZIP transcription factors, outside of the closest homologs to *VRS1*, regulate development via growth suppression (20, 23, 24, 27–33). Indeed, a *VRS1* homolog separated by *ca.* 70 My of divergence, *GRASSY TILLERS1* (*GT1*), suppresses the growth of axillary meristems and pistils in maize (27, 34, 35). In barley, *HvGT1* delays preanthesis tip degeneration, resulting in a higher final spikelet number (33). In rice (*Oryza sativa*), an ortholog of *GT1* also represses axillary meristem outgrowth (36). In the eudicots, orthologs of *GT1* and *VRS1* suppress growth in many different species and contexts, including regulating growth and development of axillary meristems in arabidopsis (28) and pollen-producing organs in persimmon (*Diospyros lotus*) and melon (*Cucumis melo*) (29, 37). Other more distantly related class I HD-Zips suppress growth in leaf margins in *Cardamine hirsuta* and cotton (*Gossypium hirsutum*) (30–32). These eudicots are separated by 160 My of evolution from the grasses, yet class I HD-ZIPs retain their capacity for growth repression (38). Together, these data suggest that class I HD-ZIP gene transcription factors maintain a conserved and shared function of negatively regulating growth.

Here, we used CRISPR-Cas9 gene editing and mutant analysis to ask what conserved roles the homologs of key domestication genes *VRS1* and *GT1* have in regulating growth repression in maize and brachypodium. We found that these genes impact critical domestication traits and have deeply conserved roles in growth repression. Thus, guided by evolution, these genes represent ideal gene editing targets for the continued improvement of a broad range of crops and their wild relatives.

## Results

***VRS1* and *GT1* Homologs Have Complex Evolutionary Histories.** To understand how many *VRS1*- and *GT1*-like genes might influence growth repression in the grasses, we first examined the evolutionary histories of *VRS1* and *GT1* homologs (Fig. 1*A* and *SI Appendix*, Fig. S1). Gene duplications are prevalent in these gene lineages. An ancient duplication in the lineage leading to the grass family likely generated the two main *VRS1*- and *GT1*-like lineages (35, 39). Wheat and barley share a second duplication that excludes brachypodium. Therefore, the barley genes *VRS1* and *HvHOX2* are co-orthologous to a single gene in brachypodium (40). Similarly, because of an independent duplication in a lineage leading to maize, two maize genes are separately co-orthologous with *VRS1* and *HvHOX2* (41). To account for these complex relationships, we refer to the maize *VRS1* and *HvHOX2* co-orthologs as *VRS1-LIKE1* (*VRL1*) and *VRL2* and the brachypodium ortholog as *BdVRL1*.

***GT1* and *VRL1* Repress Growth in Axillary Meristems and Ear Flowers.** To determine the role of *VRL1* in the grasses, we examined the *gt1*, *vrl1*, and *gt1; vrl1* phenotypes in maize transposon insertion lines and in mutants generated via CRISPR-Cas9 gene editing (Fig. 1*B*). *gt1* maize mutants have more tillers (basal branches) and ears compared to wild type (Fig. 1 *C*, *D*, and *F*; 27). In contrast, *vrl1* single mutants had more ears (but not more tillers) than wild-type plants (Fig. 1 *C*, *D*, and *F*). To dissect the genetic interaction between *GT1* and *VRL1*, we made *gt1; vrl1* double mutants, which had even more ears and tillers than single mutants (Fig. 1 *C*, *D*, and *F*). In addition, *gt1; vrl1* tillers were longer than those of *gt1* (Fig. 1*E*). Together, these data suggest that *GT1* and *VRL1* are acting jointly in axillary meristem growth suppression in maize.

Because of the known roles of *GT1* and *VRS1* homologs in floral organ growth suppression (20, 23, 27, 29, 33, 34), we also investigated changes in maize flowers. Maize has two inflorescence types: the staminate tassel at the apex of the plant and the pistillate ears in the axils of upper leaves. In wild-type maize ears, spikelets initiate pairs of upper and lower flowers. However, the lower flower aborts, in part because of pistil suppression (Fig. 2 *A* and *B*). This is also the case in *gt1* and *vrl1* single mutants (Fig. 2 *C* and *D*). However, in *gt1; vrl1* double mutants, the pistil of the lower flower did not abort (Fig. 2 *E*, *F*, and *H*). Although this led to misrowing in *gt1; vrl1* ears, there was not a significant change in kernel row number (*SI Appendix*, Fig. S2). When *gt1*; *vrl1*/+ plants were examined, we found partially developed lower flower pistils in some of the spikelets, suggesting a dosage effect (*SI Appendix*, Fig. S3 *A* and *C*). Together, these data show that *GT1* and *VRL1* both act to repress growth of the pistil in lower ear flowers in maize.

We also investigated the floral phenotype in *gt1; vrl1* tassels. When initially examined, *gt1-mum2* and *gt1-mum2; vrl1-mum1* mutants bore long silks in tassel flowers (*SI Appendix*, Fig. S4). However, upon backcrossing to B73, the strength of this phenotype decreased to that described for *gt1* (27, 34). This suggests that the silky tassel phenotypes of double mutants are due to background modifiers that are not present in B73 (*SI Appendix*, Fig. S4). This also indicates that while *GT1* suppresses pistil growth in both tassels and ears (27, 34), *VRL1* activity is limited to pistils in ear flowers.

In addition to derepressed pistils, *gt1; vrl1* double mutants had extra organs in both upper and lower flowers (Fig. 2 *E*–*G*). These organs were similar to stamens, bearing structures that resembled anthers and filaments, but did not produce pollen. These extra organs were not observed in single mutants (Fig. 2 *C* and *D* and *SI Appendix*, Fig. S3 *A* and *B*). Stamens are typically suppressed in ear flowers. Based on the position and shape of these extra organs, we hypothesize that these were partially derepressed stamens.

We further asked which genes *GT1* and *VRL1* regulate. We performed RNA-seq of maize ear inflorescences in wild type, *gt1*, *vrl1*, and *gt1; vrl1* individuals from a segregating population, and determined which genes were differentially expressed (*SI Appendix*, Table S2). A total of 219 genes were differentially expressed between wild type and all the mutant genotypes in the immature ear stage, with 111 unique to the wild type-to-*gt1; vrl1* comparison (Dataset S2 and *SI Appendix*, Fig. S5*A*). Since *gt1; vrl1* double mutants have a strong ear phenotype, we investigated the genes that were uniquely differentially expressed in *gt1; vrl1* ears (*SI Appendix*, Fig. S5*B*). A large number of transcription factors, including C2H2, bZIP, homeodomain, MYB, and WRKY transcription factors, were

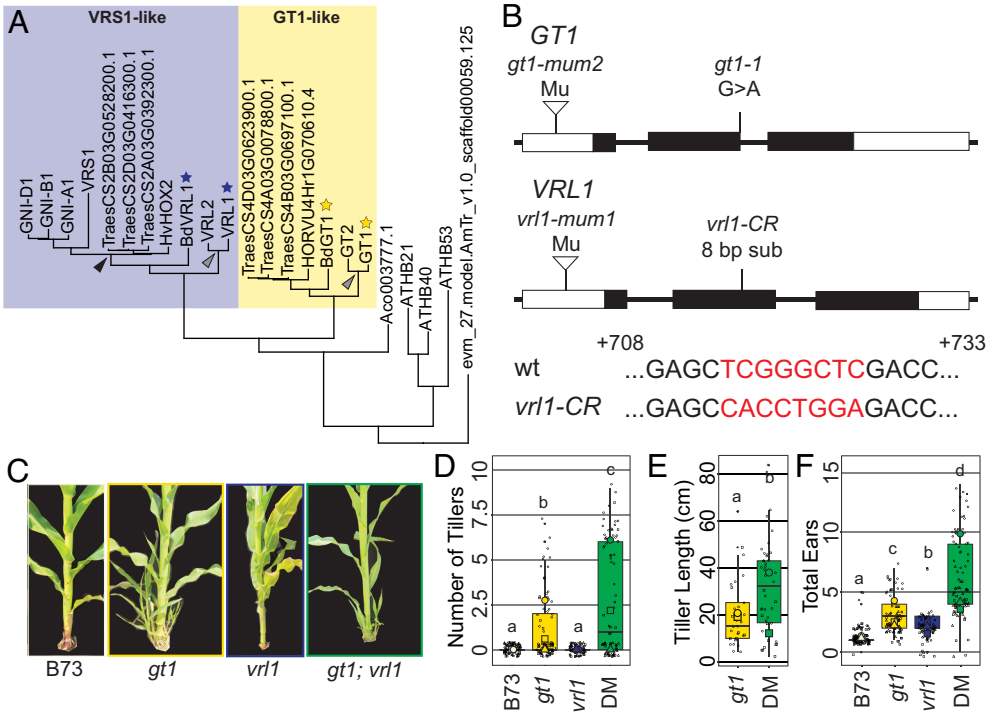


**Fig. 1.** *VRL1* enhances *GT1* lateral growth repression. (*A*) Gene tree showing the evolutionary history of the *GT1* (yellow box) and *VRS1* (blue box) lineages of the class I HD-ZIPs. The black arrow points to the node at which the *VRS1* and *HvHOX2* lineages diverged. The gray arrows point to the nodes at which the maize-specific duplication led to the divergence of *GT1* and *GT2* and of *VRL1* and *VRL2*. Stars highlight genes used in this study. Bootstrap support values are available in *SI Appendix*, Fig. S1. (*B*) Mutant lesions used in this study. For *GT1*, a Mu-insertion line and the previously described *gt1-1* allele were used. For *VRL1*, a Mu-insertion line and a CRISPR mutant were used. An alignment of the wild-type *VRL1* allele and the *vrl1-CR* allele is provided. (*C*) Tillering in maize plants, left to right: wild type, *gt1*, *vrl1*, *gt1*; *vrl1*. Colored outlines correspond to bar plot colors in panels *D*–*F*. (*D*) Quantification of the number of tillers per plant. (*E*) Quantification of tiller length per plant. (*F*) Quantification of the number of ears produced per plant. In *D*–*F*, DM = double mutant (*gt1; vrl1*), square = 2019 field, circle = 2020 field, triangle = 2021 field. Large shapes are year means, small points are individual plants. Different letters above bars correspond to significantly different means (Tukey's HSD Test, $P < 0.05$).

differentially expressed, as were receptors, sugar transporters associated with programmed cell death, and genes associated with floral development (*SI Appendix*, Fig. S5*B* and Dataset S2). Gene Ontology (GO) enrichment analysis of the Biological Processes category revealed that those genes that were upregulated in *gt1; vrl1* double mutant versus the wild type showed enrichment for positive regulation of various biosynthetic processes (Dataset S3), while those genes that were down-regulated in *gt1; vrl1* versus wild type were enriched for transmembrane transport and various catabolic processes (Dataset S3). These individual genes and GO categories

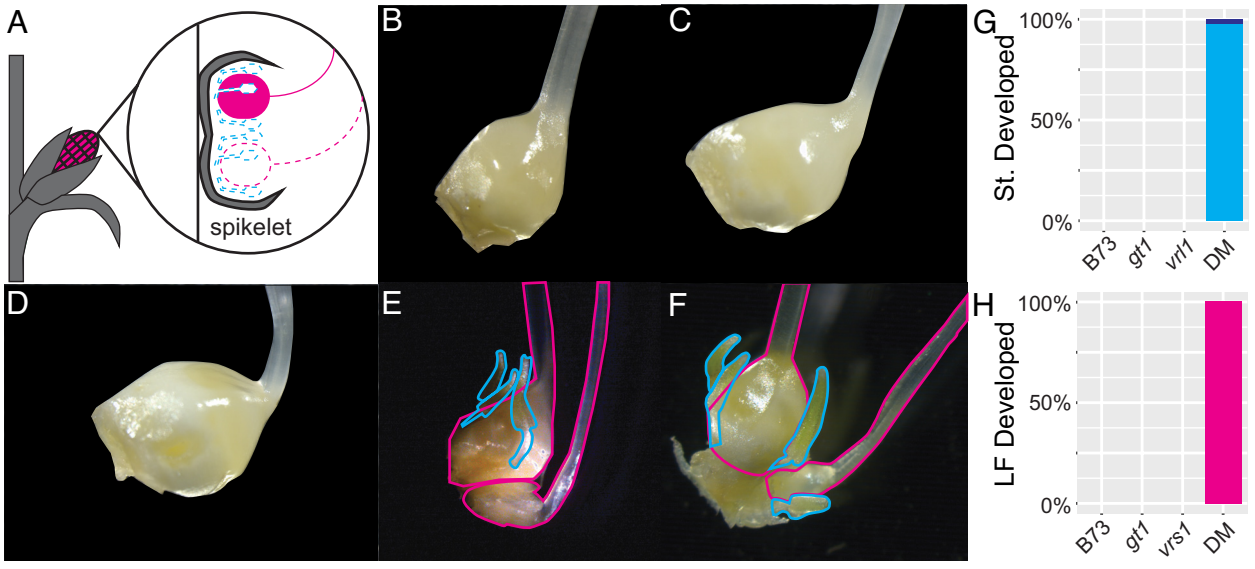


**Fig. 2.** *VRL1* and *GT1* regulate repression of reproductive structures in the ear spikelets. (*A*) Diagram of maize ear spikelet development. In normal ears, the lower flower pistil (pink) and the stamens (cyan) of both flowers are repressed (dotted line) while the upper flower pistil develops (solid). (*B*–*F*) Images of developing maize ear spikelets with palea, lemma, and lodicules removed. B, inbred line B73. (*C*) *gt1*. (*D*) *vrl1*. (*E*) *gt1-mum2; vrl1-mum1*. (*F*) *gt1-1; vrl1-CR*. (*G*) Quantification of the number of ear spikelets with stamen-like structures. No wild-type, *gt1*, or *vrl1* plants developed stamen-like structures. All *gt1; vrl1* plants showed stamen-like structures in both flowers (cyan) except one, which showed stamen-like structures in the upper flower only (dark blue). (*H*) Quantification of the number of ear spikelets with developed lower flower pistils. No wild-type, *gt1*, or *vrl1* plants developed lower flower pistils. All *gt1; vrl1* plants developed lower flower pistils.

align with the possibility that with the failure to repress development of the lower flower in *gt1; vrl1* plants, there would be reduced expression of genes associated with breaking down and reusing the cellular components from the normally repressed floral organs. This may be due to interactions with the metabolic homoeostasis regulators SnRK1 and trehalose (42–44); *GT1* interacts genetically with the trehalose phosphate phosphatase (TPP) *RA3* and may connect to plant metabolism through this link (34).

***GT1* and *VRS1* Homologs Maintain Growth Repression Functions over Deep Time.** To further test our hypothesis that *GT1* and *VRS1* homologs have conserved roles in regulating growth repression, we made CRISPR-Cas9 knockouts of their homologs in the tractable experimental system brachypodium, which is separated from maize by *ca.* 59 My of evolution (Fig. 3 *A* and *B*; 38). While *Bdvrl1* single mutants had no strong phenotype, *Bdgt1* and *Bdgt1; Bdvrl1* both had more tillers than wild type (Fig. 3 *C*–*H*). Spikelet number and flower number were also higher in *Bdgt1; Bdvrl1* double mutants than in either single mutant or wild-type (Fig. 3 *I* and *J*). However, despite the higher number of spikelets and flowers, neither grain number nor total grain weight per plant was significantly higher in any mutants compared to wild type (Fig. 3 *K* and *L*). This suggests that *BdGT1* and *BdVRL1* play a role in repressing floral initiation and development but that there are additional genetic or environmental components that impact maturation of pollinated flowers into grains (45).

Because of the repeated evolution of roles in growth repression in this gene lineage and the growth repression phenotypes uncovered in this work, we hypothesized that this lineage of HD-ZIPs could be redirected to repress growth regardless of the developmental context. To assess whether *GT1* and *VRS1* homologs were sufficient to repress growth in heterologous developmental contexts, we expressed maize *GT1* in arabidopsis petals and stamens, using the *APETALA3* (*AP3*) promoter (46, 47) (Fig. 4*A*). If *GT1* could act as a growth repressor in a new context, we expected that this heterologous expression of *GT1* would reduce the size of petals and stamens (Fig. 4*A*). Indeed, petal length, petal width, and stamen length were all significantly reduced in the *AP3::GT1* plants compared to the control *AP3::YFP* plants (Fig. 4 *B* and *C*). Just as this growth repression module was recruited to new roles in development, the genetic module regulated by *GT1* may be redeployed to initiate growth repression via transgenic approaches, even in species separated by 160 My of evolution (38).

## Discussion

Here, we show that, despite undergoing evolutionary divergence for *ca.* 70 My, *GT1*-like and *VRS1*-like genes have broad, conserved roles in growth repression in the grasses. Although maize *vrl1* plants do not exhibit obvious phenotypes, maize *gt1; vrl1* double mutants develop more ears and more floral organs in the ear spikelets than wild type or *gt1* mutants (Figs. 1*F* and 2). Brachypodium *bdgt1; bdvrl1* double mutants had more branches, spikelets, and flowers as compared to wild type, confirming these genes' role in growth repression (Fig. 3 *H*, *I*, and *J*). Thus, *GT1*-like and *VRS1*-like genes maintain a conserved function in regulating growth suppression in the grasses. Further, ectopically expressed *GT1* reduced growth of arabidopsis floral organs, demonstrating that these genes can be used to initiate localized growth repression even across deep evolutionary timescales (Fig. 4 *B* and *C*).

Our work demonstrates that *GT1*-like and *VRS1*-like genes maintain a conserved role in growth repression, regulating similar traits across species (Figs. 1–3). However, these genes also display a propensity for recruitment to new developmental contexts, as in repression of maize flower organs (Fig. 2 *E* and *F*) (34). This repeated recruitment suggests that these genes are genetic hotspots that are recurrently deployed to sculpt plant morphology (48–50). That is, these genes regulate a conserved module of growth repression that can be recruited to new contexts within plant development. While other genes may also direct growth repression, these can be pleiotropic, regulating additional phenotypes. For example, *TEOSINTE BRANCHED1* (*TB1*) regulates both growth repression and sexual differentiation (51), whereas *GT1*-like and *VRS1*-like genes direct a phenotype limited to growth repression, although it can occur across tissues (Figs. 1–3; 20, 27). Examples from evolution (differential regulation of *LMI1* and *RCO*), domestication (*prol1.1* regulation of *GT1* in maize and teosinte), and molecular biology (*AP3::GT1* in arabidopsis; Fig. 4) show that this module may be redeployed to new contexts via gene regulatory elements (Fig. 4; 30, 31, 52, 53). Investigation and application of these regulatory elements could impact crop improvement through the directed manipulation of plant morphology by growth repression.

Gene duplication is an inherent component of *GT1/VRS1* gene lineage evolution. As shown, the *GT1* and *VRS1* lineages are the result of a genome duplication in the grasses; further duplications led to even more convoluted homologies (Fig. 1*A*). Frequently, gene duplicates are reduced to single copies over time (54). However, certain types of genes, such as those encoding transcription factors like GT1 and VRS1, are retained in higher copy numbers following whole genome duplication (55, 56). Genome duplication, through the combination of multiple genomes, initially leads to greater variation in gene content, gene expression, and gene regulation; this variation may provide the raw material upon which evolution can act, leading to a variety of functional fates for a given set of gene duplicates (57). The anciently duplicated *GT1* and *VRS1* homologs both contribute to growth repression in maize and brachypodium (Figs. 1–3). However, each gene has been independently identified as a domestication gene in separate crop species (20, 23, 27). Thus, for each crop species, one of the two gene duplicates appears to have a more important role in plant development and domestication. As we see in maize, however, the other duplicate still may retain a role in regulating domestication traits (e.g., apical dominance; Fig. 1 *D*–*F*). In the context of de novo domestication, this work supports the idea that gene editing paralogs of known domestication genes may introduce further degrees of phenotypic variation for a given trait (7).

Flower number and fertility are key yield-related traits regulated by *VRS1* and *HvGT1* in barley and *GNI1* in wheat (20, 23, 33). Here, in line with that data, the double mutants in maize and brachypodium both showed an increase in flower number (Figs. 2 *E* and *F* and 3*J* and *SI Appendix*, Fig. S2*A*). However, this increase in flowers did not lead to a change in kernel row number in maize or grain number and weight in brachypodium (Fig. 3 *K* and *L* and *SI Appendix*, Fig. S2*B*). While *GT1* and *VRS1* homologs may regulate the number of flowers that develop, additional genetic components contribute to their survival and maturation into grains. The genetic elements underlying inflorescence traits such as tissue greening, water and nutrient transport, and grain retention all interact with those underlying flower number to influence the final yield for crop species (58–63). Selection of genes regulating other inflorescence traits needs to occur concurrently with selection of *GT1* and *VRS1* homolog variants to maximize crop and de novo domesticate yields, as editing multiple loci in tandem can achieve a more complete desired phenotype (2, 3).

Gene editing of *GT1* and *VRS1* homologs represents a new tool for crop engineering and de novo domestication. Modulating

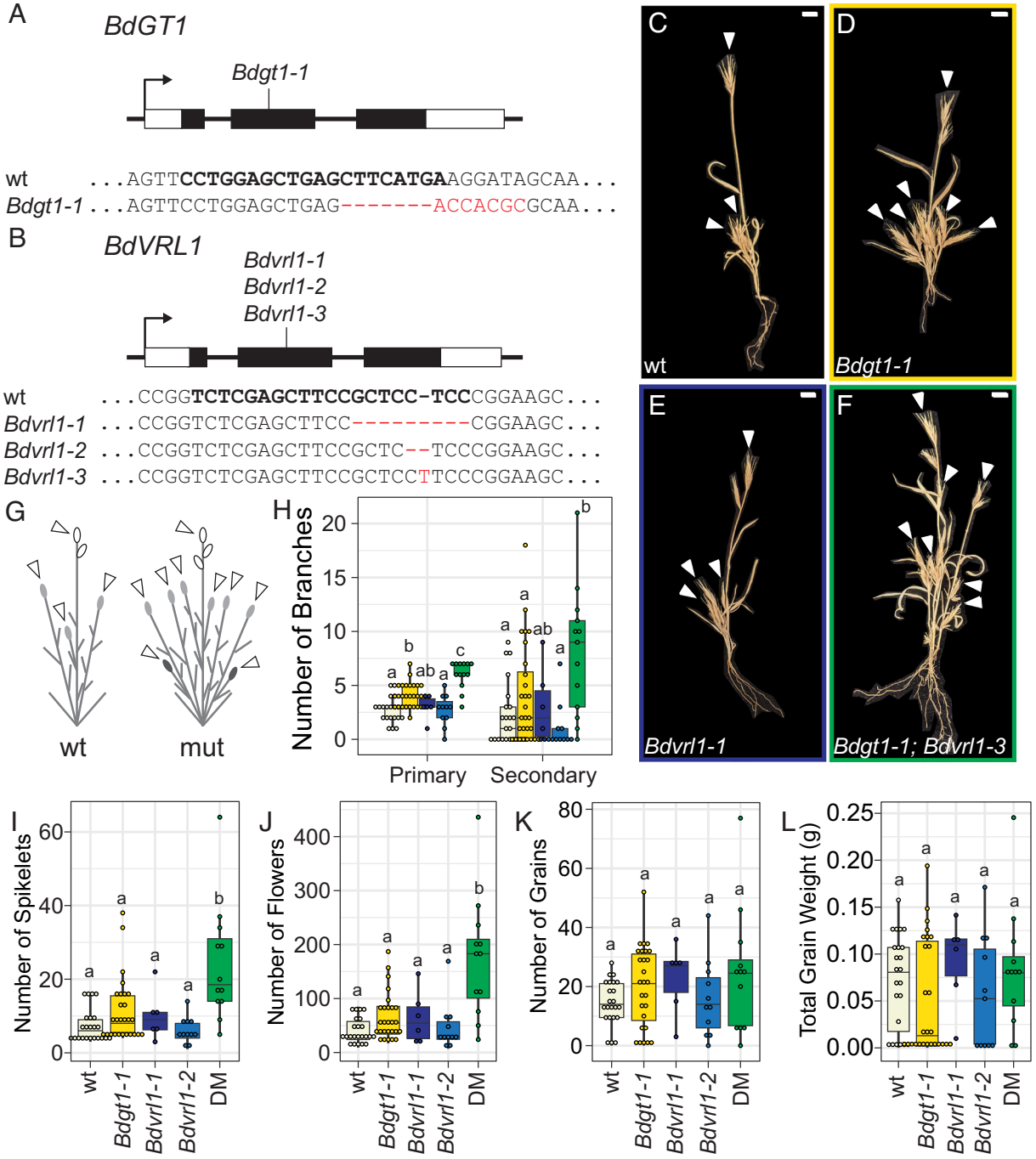


**Fig. 3.** The growth repression role of *VRS1* and *GT1* homologs is conserved in brachypodium. (*A* and *B*) *Bdgt1* and *Bdvrl1* CRISPR lesions generated in this study. In the alignment, the bold text shows the site of the spacer, and the red text shows the changes from the wild-type sequence in each mutant allele. (*C*–*F*) The branching patterns of wild-type, *Bdgt1-1*, *Bdvrl1-1*, and *Bdgt1-1; Bdvrl1-3* brachypodium. White arrows point to spikelets on branch tips. Scale bars correspond to 1 cm. (*G*) A diagram of the wild-type versus mutant brachypodium. White spikelets (ovals) are on the main axis, light gray spikelets are on the primary branches, and dark spikelets are on the secondary branches. (*H*) Quantification of the number of primary and secondary branches per plant. (*I*) Quantification of the number of spikelets per plant. (*J*) Quantification of the number of flowers per plant. (*K*) Quantification of the number of grains per plant. (*L*) Quantification of the total grain weight per plant. Despite the increase in the number of flowers in the mutants, the total grain weight was the same on average. For *H*–*L*, white = wild type, yellow = *Bdgt1*; dark blue = *Bdvrl1-1*; light blue = *Bdvrl1-2*; and green = double mutant (DM) *Bdgt1; Bdvrl1-3*. Different letters above bars correspond to significantly different means (Tukey's HSD Test, $P < 0.05$).

growth repression via edited alleles of various effect sizes could lead to the large-scale morphological changes that are necessary for the transition from wild to domesticated species or, by targeting the regulatory regions upstream of these genes, the small-scale changes necessary to improve current crops. Following evolution's guide, other genes that have conserved functions, have a history of repeated recruitment, and encode negative regulators may also be strong candidates for inclusion in the crop engineering toolkit (6, 7). Gene duplicates may also play an important role, resulting in more complex phenotypes due to redundancy and compensation (13, 15). Finally, dissecting gene regulation could provide a clearer view for how to fine-tune expression for crop engineering and de novo domestication (9, 12, 14, 16, 64). This assembled knowledge on gene evolution and development can be translated to high confidence gene editing predictions for engineering new and improved crop species.

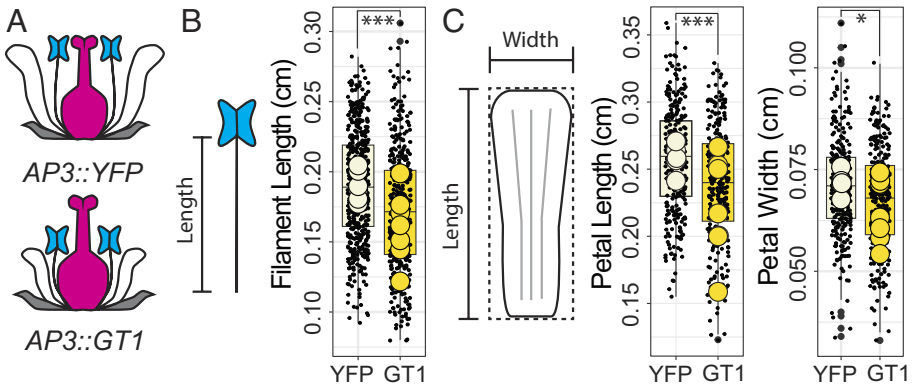


**Fig. 4.** The growth repression role of *GT1* is maintained in new contexts. (*A*) Floral diagram showing the expected phenotype of transgenic arabidopsis flowers with either *AP3::YFP* or *AP3::GT1*. With *AP3::YFP*, we expect normal growth. With *AP3::GT1*, we expect that tissues that express *AP3* normally (petals and stamens) will be smaller due to the role of *GT1* in growth repression. (*B*) Quantification of the length of filaments in transgenic arabidopsis. The filament length is shorter in *AP3::GT1* compared to *AP3::YFP* (*t* test, *P*-value = 8.943e-09). (*C*) Quantification of the petal length and width in transgenic Arabidopsis. The petal length (*t* test, *P*-value = 3.143e-08) and petal width (*t* test, *P*-value = 0.001484) are smaller in *AP3::GT1* than in *AP3::YFP*. Large circles in *B* and *C* represent plant means.

## Materials and Methods

**Gene Tree Inference.** Protein sequences of GT1, VRS1, and known homologs were used as a BLASTP query against a peptide database of 30 plant genomes available on Phytozome plus the *D. lotus* and *C. hirsuta* genome websites with an e-value cut-off of 10e-30 (Dataset S1). The peptide sequences that met the cut-off were aligned using MAFFT (65). The alignment was filtered with noisy (66). A model selection test was performed, and a tree was constructed in IQ-TREE 2 (67) and visualized using the R package ggtree (68). The outgroups for the tree were three arabidopsis HD-ZIP proteins from classes II, III, and IV [AT3G60390.1 (homeobox leucine zipper protein 3; HAT3), AT5G60690.1 (REVOLUTA; REV), and AT1G79840.2 (GLABRA2; GL2)].

**Maize Plant Materials and Growth Conditions.** Maize mutants with Mutator transposon insertions in the 5′ UTRs of *gt1* (Zm00001d028129) and one of the co-orthologous maize *vrs1* loci (Zm00001d021934), here called *vrs1-like1 (vrl1)*, were identified via a reverse genetics screen as in ref. 69. These alleles were designated *gt1-mum2* and *vrl1-mum1*. Genotyping of *gt1-mum2* and *vrl1-mum1* alleles was performed via triplex PCR with a MuTIR primer and two gene-specific primers (*SI Appendix*, Table S1).

Spacers targeting the maize homologs of *GT1* and *VRS1* were designed, assembled into pENTR, and Gateway cloned into the Cas9-containing plasmid pMCG1005-Cas9 (70). This construct was transformed into *Agrobacterium tumefaciens* strain EHA101. Plant transformation was performed at the Iowa State University Plant Transformation Facility (Ames, IA) into the Hill background. Regenerated plantlets were screened for herbicide resistance to detect successful transformants. CRISPR-Cas9 edited mutants of *vrl1-CR* were genotyped via PCR and Sanger sequencing. Spacer sequences and primers are available in *SI Appendix*, Table S1.

Plants for vegetative and reproductive phenotyping were grown at the University of Massachusetts Amherst Crop and Animal Research and Education Farm in South Deerfield, MA (~42°29′N, 72°35′W). Plants for RNA-seq were grown at the College of Natural Sciences and Education Greenhouse on the UMass Amherst campus under long day conditions (16 h light, 8 h dark) at 28 °C.

**Maize Phenotyping.** We measured phenotypes in maize inbred line B73 and in *gt1-mum2*, *vrl1-mum1*, and *gt1-mum2; vrl1-mum1* plants in their native background. Plants for phenotyping were grown in four blocks for 3 y (2018, 2019, and 2020). For each plant in each row, tiller number, tiller length, plant height, ears at each node, silks in tassels, and derepressed lower flowers were counted or measured. For counting derepressed lower flowers and floral organs, 10 spikelets per plant, four plants per genotype, were examined under the dissecting microscope. To establish whether tassel silks were a background effect, *gt1-mum2; vrl1-mum1* plants were backcrossed into the B73 inbred background four times, selfed, and phenotyped. Previously described *gt1-1* (27) and CRISPR allele *vrl1-CR* were used to confirm initially observed phenotypes. These alleles plus CRISPR alleles were used to phenotype the presence of stamen-like structure in maize ears.

**CRISPR-Cas9 Gene Editing in Brachypodium.** Spacers targeting *BdGT1* (Bradi1g71280) and *BdVRL1* (Bradi1g23460) were designed using the software CRISPOR (71). These spacers were synthesized and assembled into a guide RNA construct using the MoClo system (72–74). The resulting construct was Gateway cloned into pOsCas9_RC_of_L, a Cas9- and hygromycin resistance-containing expression vector (75, 76). This construct was introduced to brachypodium Bd21-3 embryogenic callus via *Agrobacterium*-mediated transformation using strain AGL1 (77). Calli were screened for successful transformation via hygromycin resistance and were regenerated into plantlets. *Bdgt1* and *Bdvrl1* alleles were genotyped via PCR and Sanger sequencing. Spacer sequences and primers are available in *SI Appendix*, Table S1.

Brachypodium plants were grown in growth chambers either at the Morrill Greenhouse on the UMass Amherst campus or in the Bartlett lab. All plants were grown under long day conditions (20 h light, 4 h dark) at 24 °C.

**RNA-Seq Sampling and Analysis.** From a family segregating for *gt1-mum2* and *vrl1-mum1* and backcrossed into B73 inbred background four times, 56 maize ears were collected and frozen in liquid nitrogen. RNA was extracted from these tissues using Qiagen RNeasy Plant Mini Kit (Qiagen), treated with DNase I, and cleaned up with Monarch RNA Cleanup Kit (10 μg) (NEB). These cleaned RNA samples were sent to Novogene for poly-A tail enrichment mRNA library preparation and 150 bp paired-end sequencing on Illumina NovaSeq (Novogene).

Sequenced RNA libraries were trimmed for quality using Trimmomatic and mapped to the *Zea mays* (maize) B73 version 5 genome using STAR 2.7.9a (78, 79). Reads mapped to genes were counted using HTSeq (80). R package RUVSeq was used to normalize the read counts using upper quartile normalization and the expression of the 5,000 least differentially expressed genes between the *gt1; vrl1* and wild-type ear samples (81). Differential expression analysis was performed among ears sized 0.7 to 1.3 cm, when lower flower repression was observed in wild-type plants, using DESeq2 (82). Gene ontology analysis was performed on differentially expressed gene sets using topGO and maize gamer annotation (83, 84).

**Arabidopsis Constructs and Transformation.** The promoter of arabidopsis *APETALA3* (*AP3*) and the coding sequence of maize *GT1* were amplified and cloned into Level 0 backbones (pICH41233 and pICH41308, respectively) using the MoClo System (72, 73) (*SI Appendix*, Table S1). Two constructs were Golden Gate cloned into kanamycin-resistant expression vector pICH86966 with the CaMV 35S terminator (pICH41414): one with the AP3 promoter driving *GT1* and one with the AP3 promoter driving *YFP* (from pICSL80014) (72, 73). These constructs were transformed into arabidopsis using the floral dip method of *Agrobacterium*-mediated transformation in strain GV3101, as in

Zhang et al. (85). Transformed arabidopsis were screened for kanamycin resistance. Resistant T0 generation plants were phenotyped for petal and stamen size in opened flowers.

**Data, Materials, and Software Availability.** Raw sequencing data are available at the National Center for Biotechnology Information BioProject PRJNA996557 (86); Code for analyses is available on GitHub (https://github.com/BartlettLab/GT1VRS1) (87).

**ACKNOWLEDGMENTS.** This work was supported by an NSF CAREER award (IOS-1652380) to M.E.B. and a USDA NIFA AFRI Postdoctoral Fellowship (2019-67012-29654) to J.P.G.

Author affiliations: [a]Biology Department, University of Massachusetts, Amherst, MA 01003; [b]Forage Seed and Cereal Research Unit, US Department of Agriculture, Agricultural Research Service, Corvallis, OR 97331; [c]Corteva Agriscience, Johnston, IA 50131; and [d]Napigen, Inc., Wilmington, DE 19803

1. A. Zsögön *et al.*, De novo domestication of wild tomato using genome editing. *Nat. Biotechnol.* **36**, 1211–1216 (2018).
2. E. Lacchini *et al.*, CRISPR-mediated accelerated domestication of African rice landraces. *PLoS One* **15**, e0229782 (2020).
3. C.-T. Kwon *et al.*, Rapid customization of Solanaceae fruit crops for urban agriculture. *Nat. Biotechnol.* **38**, 182–188 (2020).
4. H. Yu *et al.*, A route to de novo domestication of wild allotetraploid rice. *Cell* **184**, 1156–1170.e14 (2021).
5. Z. H. Lemmon *et al.*, Rapid improvement of domestication traits in an orphan crop by genome editing. *Nat Plants* **4**, 766–770 (2018).
6. Y. Eshed, Z. B. Lippman, Revolutions in agriculture chart a course for targeted breeding of old and new crops. *Science* **366**, eaax0025 (2019).
7. M. E. Bartlett, B. T. Moyers, J. Man, B. Subramaniam, N. P. Makunga, The power and perils of de novo domestication using genome editing. *Annu. Rev. Plant Biol.* **74**, 727–750 (2022).
8. L. DeHaan *et al.*, Roadmap for accelerated domestication of an emerging perennial grain Crop. *Trends Plant Sci.* **25**, 525–537 (2020).
9. S. Curtin, Y. Qi, L. E. P. Peres, A. R. Fernie, A. Zsögön, Pathways to de novo domestication of crop wild relatives. *Plant Physiol.* **188**, 1746–1756 (2022).
10. D. P. Wickland, Y. Hanzawa, The *FLOWERING LOCUS T/TERMINAL FLOWER 1* gene family: Functional evolution and molecular mechanisms. *Mol. Plant* **8**, 983–997 (2015).
11. J. C. Fletcher, The CLV-WUS stem cell signaling pathway: A roadmap to crop yield optimization. *Plants* **7**, 87 (2018).
12. L. Liu *et al.*, Enhancing grain-yield-related traits by CRISPR-Cas9 promoter editing of maize *CLE* genes. *Nat Plants* **7**, 287–294 (2021).
13. C.-T. Kwon *et al.*, Dynamic evolution of small signalling peptide compensation in plant stem cell control. *Nat Plants* **8**, 346–355 (2022).
14. D. Rodríguez-Leal, Z. H. Lemmon, J. Man, M. E. Bartlett, Z. B. Lippman, Engineering quantitative trait variation for crop improvement by genome editing. *Cell* **171**, 470–480.e8 (2017).
15. D. Rodriguez-Leal *et al.*, Evolution of buffering in a genetic circuit controlling plant stem cell proliferation. *Nat. Genet.* **51**, 786–792 (2019).
16. X. Wang *et al.*, Dissecting cis-regulatory control of quantitative trait variation in a plant stem cell circuit. *Nat Plants* **7**, 419–427 (2021).
17. P. D. Hsu, E. S. Lander, F. Zhang, Development and applications of CRISPR-Cas9 for genome engineering. *Cell* **157**, 1262–1278 (2014).
18. S. Soyk *et al.*, Variation in the flowering gene *SELF PRUNING 5G* promotes day-neutrality and early yield in tomato. *Nat. Genet.* **49**, 162–168 (2017).
19. L. Pnueli *et al.*, The *SELF-PRUNING* gene of tomato regulates vegetative to reproductive switching of sympodial meristems and is the ortholog of *CEN* and *TFL1*. *Development* **125**, 1979–1989 (1998).
20. T. Komatsuda *et al.*, Six-rowed barley originated from a mutation in a homeodomain-leucine zipper I-class homeobox gene. *Proc. Natl. Acad. Sci. U.S.A.* **104**, 1424–1429 (2007).
21. S. Sakuma, T. Schnurbusch, Of floral fortune: Tinkering with the grain yield potential of cereal crops. *New Phytol.* **225**, 1873–1882 (2020).
22. S. Sakuma *et al.*, Extreme suppression of lateral floret development by a single amino acid change in the VRS1 transcription factor. *Plant Physiol.* **175**, 1720–1731 (2017).
23. S. Sakuma *et al.*, Unleashing floret fertility in wheat through the mutation of a homeobox gene. *Proc. Natl. Acad. Sci. U.S.A.* **116**, 5182–5187 (2019).
24. T. Kelliher *et al.*, One-step genome editing of elite crop germplasm during haploid induction. *Nat. Biotechnol.* **37**, 287–292 (2019).
25. V. Thirulogachandar *et al.*, Leaf primordium size specifies leaf width and vein number among row-type classes in barley. *Plant J.* **91**, 601–612 (2017).
26. M. Zwirek, R. Waugh, S. M. McKim, Interaction between row-type genes in barley controls meristem determinacy and reveals novel routes to improved grain. *New Phytol.* **221**, 1950–1965 (2019).
27. C. J. Whipple *et al.*, *grassy tillers1* promotes apical dominance in maize and responds to shade signals in the grasses. *Proc. Natl. Acad. Sci. U.S.A.* **108**, E506–E512 (2011).
28. E. González-Grandío *et al.*, Abscisic acid signaling is controlled by a *BRANCHED1/HD-ZIP I* cascade in Arabidopsis axillary buds. *Proc. Natl. Acad. Sci. U.S.A.* **114**, E245–E254 (2017).
29. T. Akagi, I. M. Henry, R. Tao, L. Comai, A Y-chromosome–encoded small RNA acts as a sex determinant in persimmons. *Science* **346**, 646–650 (2014).
30. D. Vlad *et al.*, Leaf shape evolution through duplication, regulatory diversification, and loss of a homeobox gene. *Science* **343**, 780–783 (2014).
31. F. Vuolo *et al.*, Coupled enhancer and coding sequence evolution of a homeobox gene shaped leaf diversity. *Genes Dev.* **30**, 2370–2375 (2016).
32. R. J. Andres *et al.*, Modifications to a *LATE MERISTEM IDENTITY1* gene are responsible for the major leaf shapes of Upland cotton (Gossypium hirsutum L.). *Proc. Natl. Acad. Sci. U.S.A.* **114**, E57–E66 (2017).
33. N. Shanmugaraj *et al.*, Multilayered regulation of developmentally programmed pre-anthesis tip degeneration of the barley inflorescence. *Plant Cell* **35**, 3973–4001 (2023).
34. H. Klein *et al.*, Recruitment of an ancient branching program to suppress carpel development in maize flowers. *Proc. Natl. Acad. Sci. U.S.A.* **119**, e2115871119 (2022).
35. A. H. Paterson, J. E. Bowers, B. A. Chapman, Ancient polyploidization predating divergence of the cereals, and its consequences for comparative genomics. *Proc. Natl. Acad. Sci. U.S.A.* **101**, 9903–9908 (2004).
36. V. Kumar *et al.*, Tiller outgrowth in rice (Oryza sativa L.) is controlled by *OsGT1*, which acts downstream of *FC1* in a *PhyB*-independent manner. *J. Plant Biol.* **64**, 417–430 (2021).
37. D. Rashid *et al.*, Ethylene produced in carpel primordia controls *CmHB40* expression to inhibit stamen development. *Nat Plants* **9**, 1675–1687 (2023).
38. S. Kumar, G. Stecher, M. Suleski, S. B. Hedges, TimeTree: A resource for timelines, timetrees, and divergence times. *Mol. Biol. Evol.* **34**, 1812–1819 (2017).
39. M. R. McKain *et al.*, A phylogenomic assessment of ancient polyploidy and genome evolution across the Poales. *Genome Biol. Evol.* **8**, 1150–1164 (2016).
40. S. Sakuma, M. Pourkheirandish, T. Matsumoto, T. Koba, T. Komatsuda, Duplication of a well-conserved homeodomain-leucine zipper transcription factor gene in barley generates a copy with more specific functions. *Funct. Integr. Genomics* **10**, 123–133 (2010).
41. Z. Swigonová *et al.*, Close split of sorghum and maize genome progenitors. *Genome Res.* **14**, 1916–1923 (2004).
42. E. Baena-González, J. Hanson, Shaping plant development through the SnRK1-TOR metabolic regulators. *Curr. Opin. Plant Biol.* **35**, 152–157 (2017).
43. A.Y.-L. Tsai, S. Gazzarrini, Trehalose-6-phosphate and SnRK1 kinases in plant development and signaling: The emerging picture. *Front. Plant Sci.* **5**, 119 (2014).
44. J. Van Leene *et al.*, Mapping of the plant SnRK1 kinase signalling network reveals a key regulatory role for the class II T6P synthase-like proteins. *Nat Plants* **8**, 1245–1261 (2022).
45. Z. Chen, A. Gallavotti, Improving architectural traits of maize inflorescences. *Mol. Breed.* **41**, 21 (2021).
46. T. Jack, L. L. Brockman, E. M. Meyerowitz, The homeotic gene *APETALA3* of Arabidopsis thaliana encodes a MADS box and is expressed in petals and stamens. *Cell* **68**, 683–697 (1992).
47. R. S. Lamb, T. A. Hill, Q.K.-G. Tan, V. F. Irish, Regulation of *APETALA3* floral homeotic gene expression by meristem identity genes. *Development* **129**, 2079–2086 (2002).
48. M. E. James, T. Brodribb, I. J. Wright, L. H. Rieseberg, D. Ortiz-Barrientos, Replicated evolution in plants. *Annu. Rev. Plant Biol.* **74**, 697–725 (2023).
49. D. L. Stern, V. Orgogozo, Is genetic evolution predictable? *Science* **323**, 746–751 (2009).
50. T. Uller, A. P. Moczek, R. A. Watson, P. M. Brakefield, K. N. Laland, Developmental bias and evolution: A regulatory network perspective. *Genetics* **209**, 949–966 (2018).
51. J. Doebley, A. Stec, L. Hubbard, The evolution of apical dominance in maize. *Nature* **386**, 485–488 (1997).
52. D. M. Wills *et al.*, From many, one: Genetic control of prolificacy during maize domestication. *PLoS Genet.* **9**, e1003604 (2013).
53. Z. Dong *et al.*, The regulatory landscape of a core maize domestication module controlling bud dormancy and growth repression. *Nat. Commun.* **10**, 3810 (2019).
54. J. C. Schnable, N. M. Springer, M. Freeling, Differentiation of the maize subgenomes by genome dominance and both ancient and ongoing gene loss. *Proc. Natl. Acad. Sci. U.S.A.* **108**, 4069–4074 (2011).
55. J. A. Birchler, R. A. Veitia, Gene balance hypothesis: Connecting issues of dosage sensitivity across biological disciplines. *Proc. Natl. Acad. Sci. U.S.A.* **109**, 14746–14753 (2012).
56. G. Blanc, K. H. Wolfe, Functional divergence of duplicated genes formed by polyploidy during Arabidopsis evolution. *Plant Cell* **16**, 1679–1691 (2004).
57. G. Nieto Feliner, J. Casacuberta, J. F. Wendel, Genomics of evolutionary novelty in hybrids and polyploids. *Front. Genet.* **11**, 792 (2020).
58. A. R. Durbak *et al.*, Transport of boron by the *tassel-less1* aquaporin is critical for vegetative and reproductive development in maize. *Plant Cell* **26**, 2978–2995 (2014).
59. M. Chatterjee *et al.*, The boron efflux transporter ROTTEN EAR is required for maize inflorescence development and fertility. *Plant Cell* **26**, 2962–2977 (2014).
60. Y. Huang *et al.*, A molecular framework for grain number determination in barley. *Sci Adv* **9**, eadd0324 (2023).
61. Z. Dong *et al.*, *Necrotic upper tips1* mimics heat and drought stress and encodes a protoxylem-specific transcription factor in maize. *Proc. Natl. Acad. Sci. U.S.A.* **117**, 20908–20919 (2020).
62. Z. Lin *et al.*, Parallel domestication of the *Shattering1* genes in cereals. *Nat. Genet.* **44**, 720–724 (2012).
63. M. Pourkheirandish *et al.*, Evolution of the grain dispersal system in barley. *Cell* **162**, 527–539 (2015).
64. A. Hendelman *et al.*, Conserved pleiotropy of an ancient plant homeobox gene uncovered by cis-regulatory dissection. *Cell* **184**, 1724–1739.e16 (2021).
65. K. Katoh, K. Misawa, K.-I. Kuma, T. Miyata, MAFFT: A novel method for rapid multiple sequence alignment based on fast Fourier transform. *Nucleic Acids Res.* **30**, 3059–3066 (2002).
66. A. W. M. Dress *et al.*, Noisy: Identification of problematic columns in multiple sequence alignments. *Algorithms Mol. Biol.* **3**, 7 (2008).
67. B. Q. Minh *et al.*, IQ-TREE 2: New models and efficient methods for phylogenetic inference in the genomic era. *Mol. Biol. Evol.* **37**, 1530–1534 (2020).
68. G. Yu, Using ggtree to visualize data on tree-like structures. *Curr. Protoc. Bioinform.* **69**, e96 (2020).
69. R. J. Bensen *et al.*, Cloning and characterization of the maize An1 gene. *Plant Cell* **7**, 75–84 (1995).
70. S. N. Char *et al.*, An *Agrobacterium*-delivered CRISPR/Cas9 system for high-frequency targeted mutagenesis in maize. *Plant Biotechnol. J.* **15**, 257–268 (2017).
71. J.-P. Concordet, M. Haeussler, CRISPOR: Intuitive guide selection for CRISPR/Cas9 genome editing experiments and screens. *Nucleic Acids Res.* **46**, W242–W245 (2018).
72. E. Weber, C. Engler, R. Gruetzner, S. Werner, S. Marillonnet, A modular cloning system for standardized assembly of multigene constructs. *PLoS One* **6**, e16765 (2011).
73. C. Engler *et al.*, A golden gate modular cloning toolbox for plants. *ACS Synth. Biol.* **3**, 839–843 (2014).
74. J. Man, M. Bartlett, Efficient assembly of large multiplex CRISPR/Cas9 guide arrays for maize genome editing. *Bio Protoc.* **9**, e3223 (2019).

75. D. L. O'Connor *et al.*, Cross-species functional diversity within the PIN auxin efflux protein family. *Elife* **6**, e31804 (2017).
76. J. Miao *et al.*, Targeted mutagenesis in rice using CRISPR-Cas system. *Cell Res.* **23**, 1233–1236 (2013).
77. J. Vogel, T. Hill, High-efficiency *Agrobacterium*-mediated transformation of *Brachypodium distachyon* inbred line Bd21-3. *Plant Cell Rep.* **27**, 471–478 (2008).
78. A. Dobin *et al.*, STAR: Ultrafast universal RNA-seq aligner. *Bioinformatics* **29**, 15–21 (2013).
79. M. B. Hufford *et al.*, De novo assembly, annotation, and comparative analysis of 26 diverse maize genomes. *Science* **373**, 655–662 (2021).
80. S. Anders, P. T. Pyl, W. Huber, HTSeq–a Python framework to work with high-throughput sequencing data. *Bioinformatics* **31**, 166–169 (2015).
81. D. Risso, J. Ngai, T. P. Speed, S. Dudoit, Normalization of RNA-seq data using factor analysis of control genes or samples. *Nat. Biotechnol.* **32**, 896–902 (2014).
82. M. I. Love, W. Huber, S. Anders, Moderated estimation of fold change and dispersion for RNA-seq data with DESeq2. *Genome Biol.* **15**, 550 (2014).
83. A. Alexa, J. Rahnenfuhrer, topGO: Enrichment analysis for gene ontology. topGO version 2.50.0. https://bioconductor.org/packages/release/bioc/html/topGO.html. Accessed 24 February 2023.
84. K. Wimalanathan, I. Friedberg, C. M. Andorf, C. J. Lawrence-Dill, Maize GO annotation-methods, evaluation, and review (maize-GAMER). *Plant Direct* **2**, e00052 (2018).
85. X. Zhang, R. Henriques, S.-S. Lin, Q.-W. Niu, N.-H. Chua, *Agrobacterium*-mediated transformation of *Arabidopsis thaliana* using the floral dip method. *Nat. Protoc.* **1**, 641–646 (2006).
86. J. P. Gallagher *et al.*, RNA-seq of developing maize ears. NCBI Sequence Read Archive. Available at https://www.ncbi.nlm.nih.gov/bioproject/PRJNA996557. Deposited 16 July 2023.
87. J. P. Gallagher *et al.*, R code for RNA-seq analysis from "*GRASSY TILLERS* (*GT1*) and *SIX-ROWED SPIKE1* (*VRS1*) homologs share conserved roles in growth repression". Github. https://github.com/BartlettLab/GT1VRS1. Deposited 21 July 2023.